AdaViT: Adaptive Viral Tracing Informed Tractography

Charles Poirier[1,4 [0000−0001−5677−7474]], Laurent Petit[3,4 [0000−0003−2499−5367]], Joël Lefebvre[2,4 [0000−0002−6652−2130]], and Maxime Descoteaux[1,4 [0000−0002−8191−2129]]

[1] Université de Sherbrooke, Sherbrooke, QC, Canada
[2] Université du Québec à Montréal, Montréal, QC, Canada
[3] Université Bordeaux, CNRS, CEA, IMN, GIN, UMR 5293, F-33000, Bordeaux, France
[4] IRP/LIA OpTeam, CNRS Biologie et Univ. Bordeaux, France - Univ. Sherbrooke, Sherbrooke, Canada

Abstract. A major limitation of diffusion MRI tractography is its tendency to reconstruct anatomically implausible fiber trajectories. To address this issue, the integration of anatomical constraints has been suggested. In this work, we present a novel adaptive viral tracing informed tractography (AdaViT) approach. AdaViT integrates information from viral tracing experiments from the Allen Mouse Brain Connectivity Atlas to add more global context to local tractography. Starting from a list of tracking masks estimated from viral tracing projection density maps, AdaViT dynamically updates the effective tracking mask based on the previous positions of the streamline being reconstructed. This way, AdaViT constrains streamline reconstruction to regions that have greater chances of resulting in an anatomically valid connection. We first validate AdaViT on the diffusion-simulated connectivity (DiSCo) dataset and show that AdaViT reduces the occurrence of invalid connections while achieving good agreement with ground truth connectivity. We also apply AdaViT on a 50-µm isotropic resolution *ex vivo* mouse brain to disentangle a major bottleneck region located across the bridge of the corpus callosum. By integrating more global context into the local tractography algorithm, we show that AdaViT reduces the occurrence of invalid streamlines and increases the proportion of valid connections.

Keywords: Mouse brain · Anatomy · Multimodality · Tractography · Viral tracing.

1 Introduction

A major limitation of diffusion magnetic resonance imaging (dMRI) tractography is the systematic reconstruction of false positives [8,6], as has been confirmed by many tractography challenges [13]. These false positives correspond to tractography streamlines that are supported by the dMRI signal, but which do not agree with anatomical knowledge. False positives are a consequence of the coarse

resolution of dMRI with respect to the size of the axons, resulting in complex fiber configurations at the voxel level such as crossing, fanning, branching or bottleneck configurations. To resolve these problematic configurations, the inclusion of anatomical information from microscopy imaging has been suggested [18,7].

In this work, we describe a novel tractography approach, called adaptive viral tracing informed tractography (AdaViT), for addressing the false positive issue in tractography. While previous attempts have focused on locally enhancing fiber orientation distribution function (FODF) reconstruction with microscopy data [18,7], AdaViT instead integrates information from viral tracing experiments to add a more global context to local tractography. The idea behind AdaViT is to dynamically update the tracking mask based on the previous positions of the streamline being reconstructed, hence constraining streamline reconstruction to regions that have greater chances of resulting in a valid connection from an anatomical standpoint. Here, we use projection density maps from the Allen Mouse Brain Connectivity Atlas [9] (AMBCA) to generate tracking masks constraining tractography to valid regions. The AMBCA is an open resource containing thousands of mouse brain viral tracing experiments acquired in serial 2-photon excitation fluorescence microscopy, all coregistered to a common template space [17].

We evaluate the performances of AdaViT on simulated data from the diffusion-simulated connectivity (DiSCo) dataset [5] and on a 50-µm isotropic *ex-vivo* mouse brain acquisition, and show that AdaViT reduces the occurrence of invalid streamlines and increases the proportion of valid connections, by integrating more global context into local tractography.

2 Methods and material

2.1 Adaptive viral tracing informed tractography

AdaViT is an add-on tracking module that can be integrated into any conventional local probabilistic tractography algorithm. In its simplest form, a local tractography algorithm consists of the following steps: (i.) a direction is chosen based on the underlying orientation distribution function (ODF); (ii.) a fixed step is taken along that direction; (iii.) the new streamline position is tested against some stopping criterion. Usually, for step (iii.), conventional tractography algorithms determine whether streamline propagation may continue by testing that the streamline remains inside a tracking mask, imposing that propagation only happens inside white matter (WM). AdaViT replaces the tracking mask by a list of tracking masks, where each mask is a binarized projection density map from some viral tracing experiment. AdaViT is described visually in Figure 1 for three consecutive tracking steps. At each tracking step, the streamline is projected onto the voxel grid to obtain a streamline mask (a.). This streamline mask is then used to find all valid viral tracing masks. A mask is considered valid if it entirely covers the streamline mask (b.). Formally, the set M of valid tracking masks m is defined as

$$m \in M \iff S \cap m = S, \tag{1}$$

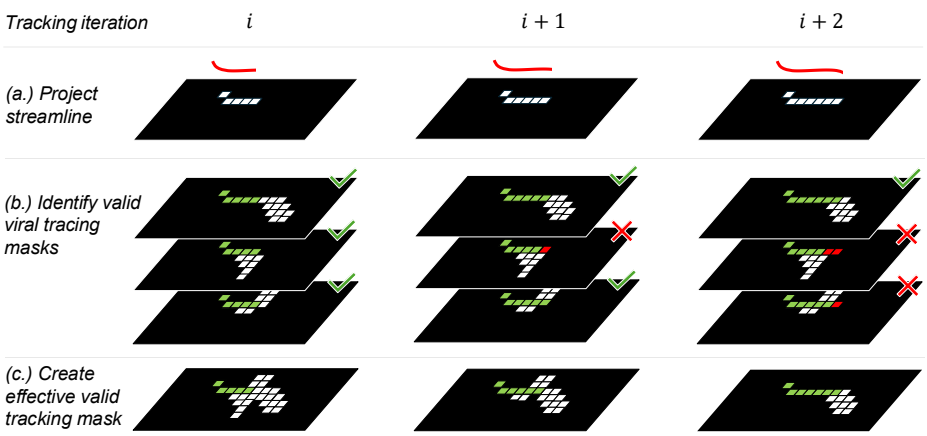

Fig. 1: Schematic description of AdaViT. At each iteration, the streamline is projected onto the voxel grid. The projection is used to determine which tracking masks are valid. Then, the current tracking mask is given by the union of all the viral tracing masks containing the streamline. Green indicates valid streamline coordinates and red indicates invalid coordinates.

where S is the streamline mask. Then, the resulting effective tracking mask T (shown in c.) is given by the union of all valid tracking masks $m \in M$:

$$T = \bigcup_{m \in M} m. \tag{2}$$

As tracking progresses, tractography becomes increasingly specific to a few tracking masks, hence enforcing that the streamline remains anatomically valid with respect to viral tracing experiments. When the set of valid tracking masks is empty, i.e. $M = \emptyset$, streamline propagation is terminated. A drawback of this simple AdaViT implementation is that streamlines have a high chance of being terminated early by taking a step supported by the diffusion signal but not supported by the global context (enforced by viral tracing constraints). To prevent this, we implement the backtracking mechanism from [14]. Backtracking attempts to save early-terminated, anatomically-implausible streamlines by retrying them from an earlier step. To do so, we define an exclusion mask corresponding to all voxels belonging to WM or ventricles. When a streamline is terminated inside an exclusion region, backtracking happens. The final Δ millimeters of the streamline are cut and tractography resumes from the earlier position. Δ is a user-controlled parameter set to $\Delta = 2$ mm in this work. AdaViT is implemented in the scilpy toolbox [11].

2.2 Material

Simulated data The Diffusion Simulated Connectivity (DiSCo) dataset [5] consists of 3 distinct simulated diffusion MRI phantoms for which the ground

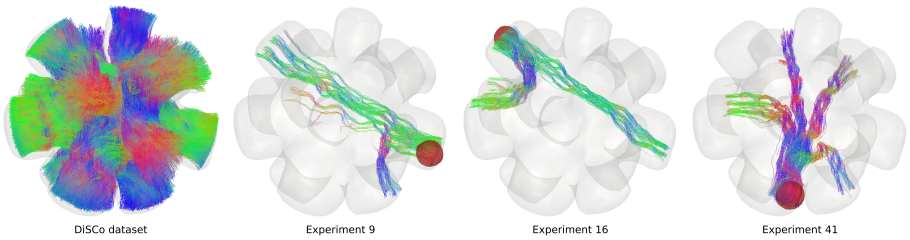

Fig. 2: Example of simulated tracing experiments from the ground-truth streamlines of the DiSCo dataset. The red spheres represent injection sites.

truth (GT) fiber trajectories are known. Each simulated phantom is available in a high and a low resolution, for varying noise levels. In this work, we use the 1-mm isotropic resolution DiSCo1 phantom with signal-to-noise ratio of 30. The GT streamlines are shown in Figure 2 (left). Streamlines are organized in bundles making connections between 16 distinct endpoint regions of interest (ROI). We reconstruct fiber ODF (FODF) from the $b = 3000$ s/mm^2 shell, using constrained-spherical deconvolution (CSD) [16] as implemented in scilpy [11]. We simulate viral tracing experiments from the GT streamlines, by first generating 80 injection sites with 2-mm radius, randomly distributed inside the endpoint ROIs. Then, for each simulated injection site, we filter the GT tractogram such that only streamlines with either end inside the injection site are kept. Example experiments are shown in Figure 2. The filtered streamlines are then projected onto the 1-mm isotropic voxel grid to obtain a simulated projection density mask. We also define an exclusion mask as the inverse of the endpoints ROI mask for backtracking invalid streamlines.

Real data Diffusion MRI data for a single *ex vivo* mouse brain was acquired using an optimized acquisition protocol from [2] (5 $b = 0$ s/mm^2; 60 $b = 3000$ s/mm^2; 50 µm isotropic resolution). Data was preprocessed and registered to Allen space using sf-mouse[5]. We estimate FODF using CSD. A WM mask is then obtained by thresholding the subject fractional anisotropy (FA) map at 0.4. The exclusion mask for backtracking is created from the union of the WM mask and a ventricles mask from the Allen template annotations.

3 Experiments

3.1 Quantitative evaluation of AdaViT on the DiSCo dataset

We run AdaViT with the 80 simulated tracking masks with step size of 0.5 mm (half-voxel), maximum curvature angle of 20°, and 10 seeds per voxel. We also compare endpoints seeding and WM seeding. For WM seeding, the seeding

[5] https://github.com/sf-mouse

mask is given by the union of all tracking masks. While, AdaViT dynamically updates the tracking mask at runtime, a simpler viral tracing informed tractography approach would consist of performing many tractography experiments, each constrained by a single tracking mask, and then concatenating the results into a single tractogram. We refer to this approach as "experiment-specific" tractography. To investigate the effect of dynamically updating the tracking mask on-the-fly, we compare AdaViT to this "experiment-specific" approach. For endpoints seeding, we use the simulated injection ROI and, for WM seeding, we use the simulated tracking mask itself. For baseline comparison, we also run local probabilistic tractography from scilpy, using the same tracking parameters and seeding masks as for AdaViT. We use the GT WM mask as the unique tracking mask. For fair comparison, we enable backtracking for all tractography methods. We then use the Tractometer [3,10] as implemented in scilpy [11] to segment the tractography outputs into valid (VB) and invalid bundles (IB) based on the GT endpoint ROIs. Streamlines are segmented based on their first and last coordinates. Because the DiSCo dataset consists of non-overlapping endpoint ROIs, each streamline is assigned to a single bundle. We also construct connectivity matrices from the resulting tractograms, using the streamline count between each pair of endpoint ROIs as the connectivity weights.

3.2 Disentangling bottlenecks in real mouse brain dMRI

We also investigate whether AdaViT helps disentangling bottlenecks in a real mouse brain dMRI acquisition. From the AMBCA, we first download the 2915 viral tracing experiments injected in grey matter, at 50 µm isotropic resolution. Then, in Allen brain atlas template space, we define a $150 \times 150 \times 150$ µm^3 bottleneck ROI located along the interhemispheric portion of the CC. Next, we identify all experiments projection density maps intersecting the ROI. The resulting experiments are binarized by thresholding the projection density maps at 1%. The masks are further processed to keep only the largest connected component, discarding any mask for which the resulting mask does not intersect the bottleneck region anymore (106 remaining experiments). The bottleneck ROI mask and all valid tracking masks are finally transformed to subject space. AdaViT is then run using 200 seeds per voxel with a step size of 0.025 mm (half-voxel) and maximum curvature angle of 20°. We seed only from the bottleneck ROI mask. For baseline comparison, we run local probabilistic tractography using the same parameters. We use the union of all tracking masks as the unique tracking mask, again enabling backtracking to keep comparison fair.

4 Results

Figure 3 compares the DiSCo GT connectivity matrix to baseline tractography, experiment-specific tractography and AdaViT for endpoints seeding (top row) and WM seeding (bottom row). Connectivity weights of 0 are shown in white. Each matrix is normalized such that the maximum weight is 1. The Pearson

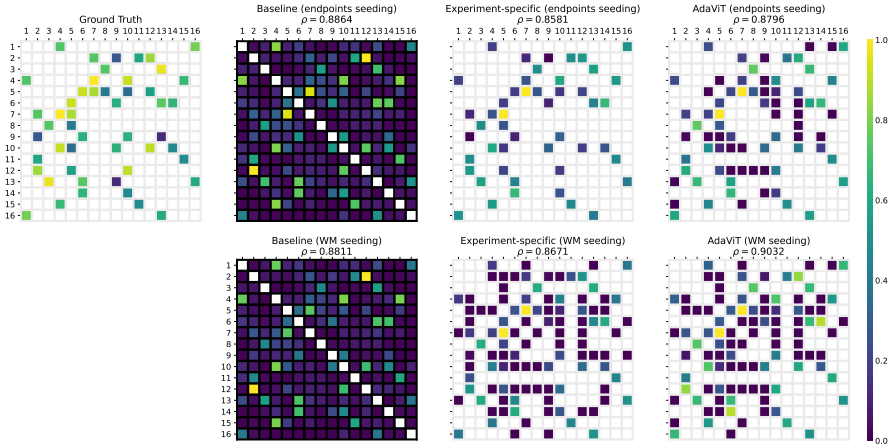

Fig. 3: DiSCo connectivity matrices comparison for different seeding strategies. Pearson correlation coefficient (ρ) is reported for each matrix.

correlation coefficients (ρ) between the estimated and GT connectivity matrices are also given. AdaViT with WM seeding achieves the highest correlation ($\rho = 0.9032$). The baseline method with endpoints seeding achieves the second best correlation ($\rho = 0.8864$), but results in non-zero connectivity weights between all pairs of endpoints. Experiment-wise tractography achieves the lowest correlations. This is because the approach constrains tractography to a single tracking mask at a time, hence biasing tractography towards orientations that remain within the tracking mask and preventing tractography from exploring the whole data. In contrast, by considering many tracking masks at the same time, AdaViT reduces this bias and better captures the whole streamlines distribution. As such, AdaViT outperforms experiment-specific tractography for both seeding strategies. Still, experiment-specific tractography with endpoints seeding is the only method estimating no false positives (FP). For both experiment-specific tractography and AdaViT, WM seeding increases correlation with GT connectivity, at the cost of an increased number of invalid connections compared to endpoints seeding. This suggests that seeding only from the injection sites hinders tractography from exploring paths that may be under-represented locally.

Figure 4 classifies the connectivity matrices from the DiSCo dataset into true positive (TP; green), true negative (TN; light green), false positive (FP; light red) and false negative (FN; red) after binarizing with a threshold of 5% their maximum value. This threshold is the same as in the original DiSCo paper [5]. The Dice coefficient for each matrix is also reported. Baseline tractography reconstructs a lot a FP, resulting in low Dice scores for both seeding strategies ($F_1 < 0.55$). Experiment-specific tractography and AdaViT generate no FP, meaning the connectivity weights for invalid connections remain below 5%. Experiment-specific and AdaViT both achieve Dice scores above 0.95, and that, for both seeding strategies. The plot in the bottom left corner shows the Dice coefficient for each method for connectivity thresholds in the range 0–12%. This

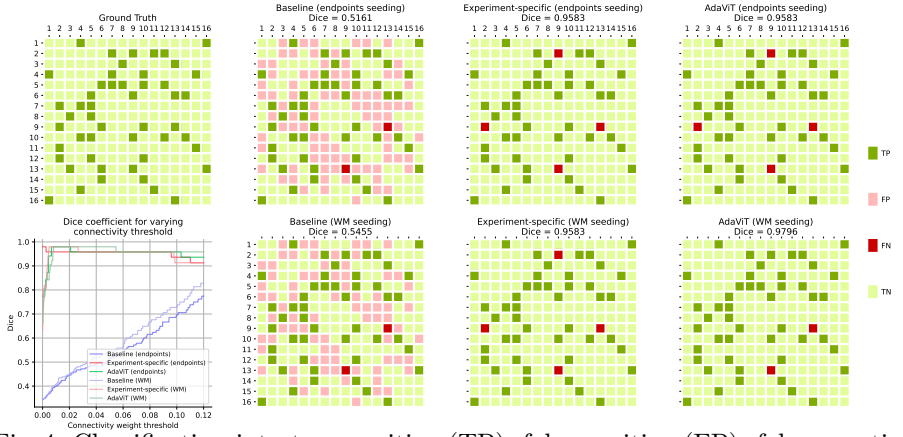

Fig. 4: Classification into true positive (TP), false positive (FP), false negative (FN), and true negative (TN) for DiSCo dataset. Dice scores are given below the methods name.

upper bound corresponds to the minimum non-zero connectivity weight in the ground truth matrix, since thresholding the ground truth above 12% would incorrectly label valid connections as missing. When the threshold is properly chosen, AdaViT and experiment-specific tractography achieve a Dice of 0.9796 for both seeding strategies. However, the baseline method remains below other methods for all threshold values.

Table 1 reports the Tractometer scores for all tractography experiments for the DiSCo dataset. Valid (VS) and invalid streamline (IS) ratios represent the proportion of output streamlines making a valid or invalid connection, respectively. The baseline method achieves the highest IS ratio for both seeding strategies, with around 30% invalid streamlines. In contrast, all viral tracing informed methods achieve VS ratios of above 99%. The seed-to-VS and seed-to-IS ratios are given by the number of valid (VS) or invalid streamlines (IS) divided by the total number of seeds. While the baseline achieves the highest seed-to-VS ratio, it also achieves the highest seed-to-IS ratio, with at least 20% of tentative streamlines making an invalid connection. Again, experiment-specific and AdaViT result in seed-to-IS ratios below 0.5% for both seeding strategies. The bundle coverage is given by the Dice score between the GT and reconstructed bun-

Table 1: Tractometer scores from the DiSCo dataset for baseline, experiment-specific and AdaViT for ROI and WM seeding.

Method	**VS ratio** (↑)	**IS ratio** (↓)	**Seed-to-VS ratio** (↑)	**Seed-to-IS ratio** (↓)	**Bundle coverage** (↑)
Baseline (endpoints)	0.6983	0.3017	0.4618	0.1995	0.7465
Baseline (WM)	0.7087	0.2913	0.5767	0.2371	0.7105
Experiment-specific (endpoints)	0.9994	0.0006	0.1837	0.0001	0.7233
AdaViT (endpoints)	0.9950	0.0050	0.2031	0.0010	0.7841
Experiment-specific (WM)	0.9947	0.0053	0.1343	0.0007	0.8401
AdaViT (WM)	0.9936	0.0064	0.3171	0.0020	0.8384

dle masks, as described in [11]. While AdaViT (WM seeding) results in slightly lower bundle coverage than experiment-specific tractography (WM seeding), it achieves a high seed-to-VS ratio (0.3171) and a low seed-to-IS ratio (0.0020).

Figure 5 compares AdaViT (left column) to standard probabilistic tractography with backtracking (baseline; right column) for a real mouse brain dMRI acquisition at 50 µm isotropic resolution for a manually segmented bottleneck region located along the interhemispheric portion of the CC. First row (left) shows three of the 106 tracking masks for AdaViT, overlayed on the subject FA map. The bottleneck ROI is represented by the white voxels. On the right, the tracking mask for baseline tractography is shown. As it is built from the union of the 106 viral tracing experiments, the tracking mask for baseline tractography covers an important portion of the brain. Both tractography methods were run from the same 200 seeding positions per voxel, for a total of 5800 seeds for each method. Second row shows the raw tractography output of each method. We report more streamlines for the baseline method than for AdaViT (4583 versus 3344). Visual comparison shows that the baseline tractogram covers more of the cortex and deep brain structures (shown by orange arrows) compared to AdaViT. We also note that baseline tractography generates longer streamlines (median length of 9.9 mm and 6.1 mm, respectively). The yellow arrow shows suspicious AdaViT streamlines that would cross the interhemispheric portion of the CC, and then project posteriorly afterward, which is improbable from an anatomical standpoint. Third row shows the result of post-filtering the tractography outputs by the seeding ROI, such that any streamline not intersecting the seeding ROI is discarded. During tracking, streamlines propagate from the seed in the forward and backward directions. Hence, after the forward pass is done, tractography restarts from the seed position for the opposite direction. However, if an invalid step is taken when doing the backward pass, backtracking will crop the end of the streamline, which may end up removing the seeding position from the resulting streamline. We see that the posteriorly-projecting streamlines in yellow don't survive the filtering, meaning they were most likely anatomically-plausible association fibers. The remaining 1081 AdaViT streamlines nicely describe transcallosal WM trajectories. We note that the baseline tractogram remains noisy even after filtering. Fourth row shows example of false positives recovered from both methods. The tractograms were segmented in MI-Brain [12] using user-defined boxes (shown in green). **A.** shows implausible fibers coming from the right cerebral peduncle and crossing the CC to project along the left side of the cortex and **B.** shows looping streamlines starting from the right hemisphere, crossing the CC and projecting back to the right hemisphere. In both cases, AdaViT results in less FP than the baseline method. Finally, last row shows the streamlines intersecting the bottleneck region and fitting entirely within one of the viral tracing masks used for AdaViT. By construction, all AdaViT streamlines fit inside a viral tracer mask. For baseline tractography, however, of the initial 3920 streamlines intersecting the bottleneck region, only 82 respect the viral tracing masks. However, it is possible that the masks do not cover the entire feasible region for a tract. Indeed, viral tracing experiments are

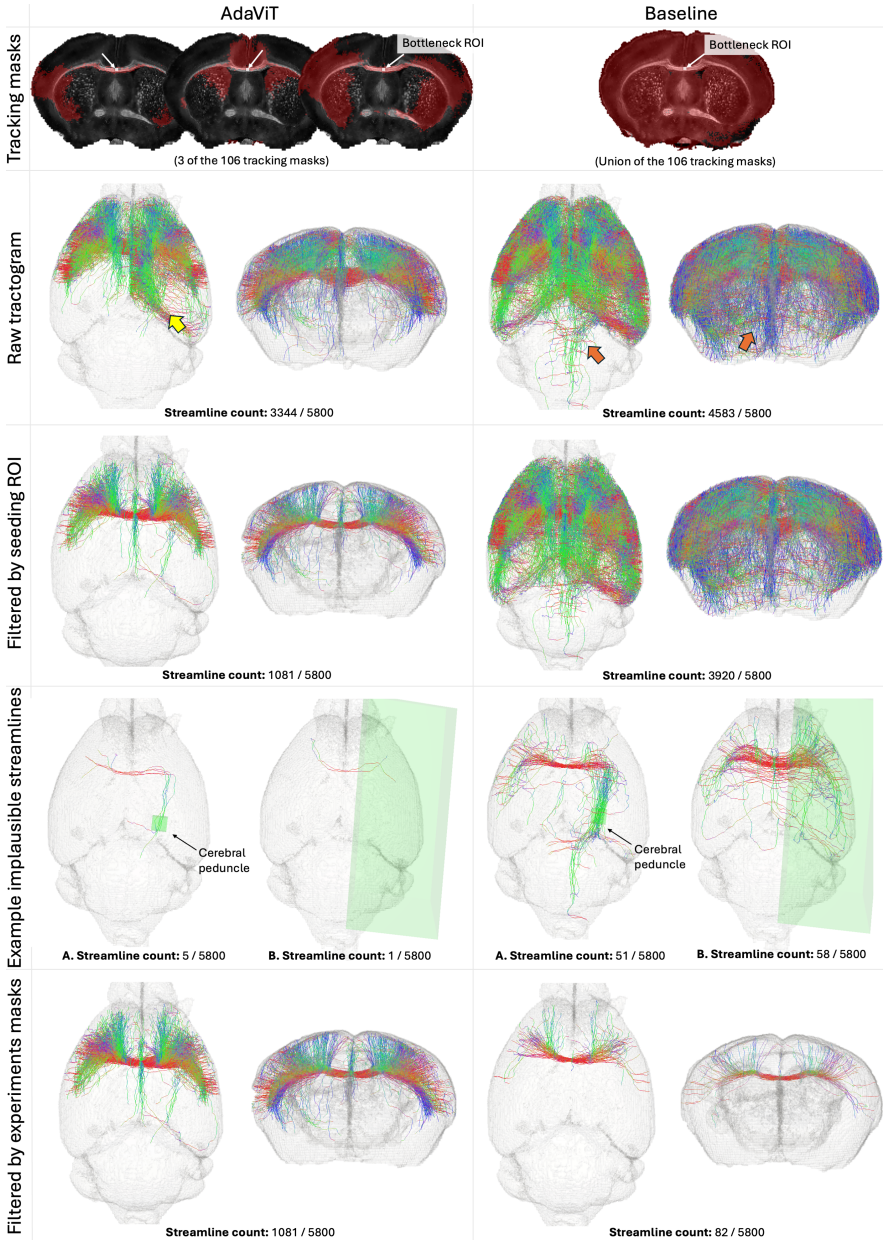

Fig. 5: AdaViT and baseline tractography for a real mouse brain dMRI acquisition at 50 µm isotropic resolution. Screenshots taken in MI-Brain.

not necessarily representative of the whole WM organization, given that only a subset of neurons emit fluorescence for a given injection experiment, influenced

by many factor including genetic mutations and kind of virus. However, while viral tracing does not necessarily explain what an invalid streamline is, it is useful for ensuring that the remaining streamlines are valid. Hence, when viral tracing masks are used to extract valid streamlines, this result shows that doing so at runtime with AdaViT results in more valid streamlines than filtering the tractogram in post-processing.

5 Discussion

We presented AdaViT, a novel approach for dMRI tractography where we dynamically update the stopping criterion based on viral tracing experiments. As we saw from simulated data, including anatomical context from viral tracing improves the classification Dice by reducing the occurrence of FN and FP, compared to a baseline tractography approach. Furthermore, AdaViT allows for filtering invalid streamlines directly during tracking. With backtracking, AdaViT replaces implausible streamlines by valid streamlines with respect to the viral tracing masks. As such, AdaViT reconstructs more valid streamlines than an experiment-specific approach for the same number of seeds, while keeping the proportion of invalid streamlines low compared to a baseline method. Finally, AdaViT does not modify the underlying FODF field. As such, if the diffusion signal does not support a direction which is valid with respect to the tracking mask, tracking will remain faithful to the underlying signal.

5.1 Limitations and future works

We quantitatively validated AdaViT on a single simulated dataset. We used the streamlines count as the edge weight for the connectivity measurements. However, future works should also evaluate more advanced connectivity metrics such as SIFT or COMMIT weights [15,4]. To quantify the reproducibility of the proposed method, future work should evaluate AdaViT on other versions of the DiSCo dataset, with different SNR and fiber configurations. Future works should also investigate the effect of the step size of tractography, spatial resolution and curation of the tracking masks by varying these parameters in a systematic study. In this work, the application to real data is limited to a single bottleneck ROI, to keep the number of tracking masks and seeds low. A more comprehensive validation of the method is therefore necessary to assess the applicability and impact of AdaViT for whole-brain connectivity analyses. AdaViT could be applied for whole-brain tractography by using all available AMBCA tracing experiments. However, because AMBCA experiments do not uniformly cover the brain, regions with more injections may be easier to reconstruct, as there are more candidate masks available. In particular, most AMBCA experiments were injected in the right hemisphere. Prior curation of the AMBCA data would therefore be required. It would also be useful to perform comparisons similar to those for the simulated data for whole-brain AdaViT. For example, we could estimate a "ground-truth" connectivity matrix from the AMBCA tracing

experiments against which to compare AdaViT. In [1], the authors use viral tracing masks to trim streamlines in postprocessing, instead of discarding them. It would be important to compare this approach against AdaViT. As a limitation, we note that using population data for tracking in an individual brain may not be representative of whole-brain connectivity. Also, viral tracing experiments do not explain where streamlines end. In this work, we make the hypothesis that any signal from a viral tracing experiment intersecting grey matter (GM) corresponds to an axonal termination. However, due to registration errors and partial volume, it is also possible that these GM projections are not anatomically valid. An additional contraint for AdaViT could be to enforce that a streamline ends inside a valid injection site. Also, to further increase the seed-to-VS ratio, we could use the viral tracing maps to constrain the FODF sampling to regions that would remain within a valid tracking mask.

5.2 Conclusion

AdaViT is a promising approach for integrating more anatomical constraints into tractography algorithms. While in this work we implemented AdaViT in a local probabilistic tractography approach, the method could be integrated into any existing tractography algorithm relying on spatially defined stopping criterion. Furthermore, AdaViT could be combined into existing microscopy-informed tractography approaches such as [18,7], allowing for incorporating viral tracing information across multiple stages of the tractography processing pipeline. This approach could even be applied for *in vivo* human brain tractography, e.g. by using bundle masks coming from a template, to constrain whole-brain tractography to anatomically plausible regions at runtime, requiring less filtering in postprocessing and ensuring more streamlines remain available for downstream analysis.

Acknowledgments. This work was supported by the CGRS-D Program from the Natural Sciences and Engineering Research Council of Canada (NSERC) and by the Excellence Scholarship from Unifying Neuroscience Quebec (UNIQUE). The authors thank Elise Cosenza for dMRI data acquisition and processing.

Disclosure of Interests. Financial support was provided by NSERC and UNIQUE. Maxime Descoteaux is cofounder and board member of Imeka Solutions.

References

1. Aydogan, D.B., et al.: When tractography meets tracer injections: a systematic study of trends and variation sources of diffusion-based connectivity. Brain Structure and Function **223** (2018). https://doi.org/10.1007/s00429-018-1663-8
2. Cosenza, E., et al.: An Optimised Multishot EPI Protocol for Ex Vivo Mouse Brain Diffusion MRI With Gd-DOTA Contrast Enhancement. NMR in Biomedicine **39**(4), e70270 (2026). https://doi.org/10.1002/nbm.70270

3. Côté, M.A., Girard, G., Boré, A., Garyfallidis, E., Houde, J.C., Descoteaux, M.: Tractometer: Towards validation of tractography pipelines. Medical Image Analysis **17**(7), 844–857 (2013). https://doi.org/10.1016/j.media.2013.03.009
4. Daducci, A., Dal Palù, A., Lemkaddem, A., Thiran, J.P.: COMMIT: Convex Optimization Modeling for Microstructure Informed Tractography. IEEE Transactions on Medical Imaging **34**(1), 246–257 (Jan 2015). https://doi.org/10.1109/TMI.2014.2352414, conference Name: IEEE Transactions on Medical Imaging
5. Girard, G., Rafael-Patiño, J., et al.: Tractography passes the test: Results from the diffusion-simulated connectivity (disco) challenge. NeuroImage **277**, 120231 (Aug 2023). https://doi.org/10.1016/j.neuroimage.2023.120231
6. Jbabdi, S., Johansen-Berg, H.: Tractography: Where Do We Go from Here? Brain Connectivity **1**(3), 169–183 (2011). https://doi.org/10.1089/brain.2011.0033
7. Liang, Z., Arefin, T.M., Lee, C.H., Zhang, J.: Using mesoscopic tract-tracing data to guide the estimation of fiber orientation distributions in the mouse brain from diffusion MRI. NeuroImage **270**, 119999 (2023). https://doi.org/10.1016/j.neuroimage.2023.119999
8. Maier-Hein, K.H., et al.: The challenge of mapping the human connectome based on diffusion tractography. Nature Communications **8**(1), 1349 (2017). https://doi.org/10.1038/s41467-017-01285-x
9. Oh, S.W., et al.: A mesoscale connectome of the mouse brain. Nature **508**(7495), 207–214 (2014). https://doi.org/10.1038/nature13186
10. Renauld, E., Théberge, A., Petit, L., Houde, J.C., Descoteaux, M.: Validate your white matter tractography algorithms with a reappraised ISMRM 2015 Tractography Challenge scoring system. Scientific Reports **13**(1), 2347 (2023). https://doi.org/10.1038/s41598-023-28560-w
11. Renauld, E., et al.: Tractography analysis with the scilpy toolbox. Aperture Neuro **6** (Jan 2026). https://doi.org/10.52294/001c.154022
12. Rheault, F., et al.: MI-Brain, a software to handle tractograms and perform interactive virtual dissection. Lisbon (2016)
13. Schilling, K.G., et al.: Challenges in diffusion MRI tractography - Lessons learned from international benchmark competitions. Magnetic Resonance Imaging **57**, 194–209 (Apr 2019). https://doi.org/10.1016/j.mri.2018.11.014
14. Smith, R.E., Tournier, J.D., Calamante, F., Connelly, A.: Anatomically-constrained tractography: Improved diffusion MRI streamlines tractography through effective use of anatomical information. NeuroImage **62**(3), 1924–1938 (Sep 2012). https://doi.org/10.1016/j.neuroimage.2012.06.005
15. Smith, R.E., Tournier, J.D., Calamante, F., Connelly, A.: SIFT: Spherical-deconvolution informed filtering of tractograms. NeuroImage **67**, 298–312 (Feb 2013). https://doi.org/10.1016/j.neuroimage.2012.11.049
16. Tournier, J.D., Calamante, F., Gadian, D.G., Connelly, A.: Direct estimation of the fiber orientation density function from diffusion-weighted MRI data using spherical deconvolution. NeuroImage **23**(3), 1176–1185 (2004). https://doi.org/10.1016/j.neuroimage.2004.07.037
17. Wang, Q., et al.: The Allen Mouse Brain Common Coordinate Framework: A 3D Reference Atlas. Cell **181**(4), 936–953.e20 (May 2020). https://doi.org/10.1016/j.cell.2020.04.007
18. Zhu, S., et al.: Imaging the structural connectome with hybrid MRI-microscopy tractography. Medical Image Analysis **102**, 103498 (May 2025). https://doi.org/10.1016/j.media.2025.103498